Journal of the European Ceramic Society 23 (2003) 213–220

www.elsevier.com/locate/jeurceramsoc

Study of solid solutions, with perovskite structure, for application in the field of the ceramic pigments

Y. Marinova*, J.M. Hohemberger, E. Cordoncillo, P. Escribano, J.B. Carda

Departamento de Química Inorgánica y Orgánica, Area de Química Inorgánica, Universitat JAUME I, 12071 Castellón, Spain

Received 10 April 2001; received in revised form 16 May 2002; accepted 25 May 2002

Abstract

There is a current need of different ways to obtain red colored systems. One way could be the intensification of the crystal field of the chromium(III) ion when it substitutes for aluminum(III) in the corundum structure (α-Al_2O_3). In the present work, solid solutions with perovskite structure ABO_3 were prepared in the system $Nd_{1-x}Y_xAl_{1-y}Cr_yO_3$ using both conventional solid state synthesis and coprecipitation. The synthesized structures were characterized structurally and microstructurally, thus determining the nature and purity of the resulting phases. A discussion is given in terms of crystal chemistry. Finally, the synthesized solid solutions were tested as ceramic pigments in enamels by measuring the chromatic coordinates, CIE-Lab.

Keywords: Crystal field; (Nd, Y)(Al, Cr)O_3; Perovskite; Pigments

1. Introduction

There is current interest in the ceramic industry for developing more stable pigments that present intense tonalities and which are in agreement with the technological and environmental requirements. The present investigation was directed towards developing ceramic pigments with red, intense tonality, which are very problematic at the moment. Currently, there are industrial ceramic pigments with red or reddish-brown hues, which present the following structures:[1]

- Pink malayaite, $CaSnSiO_5$:Cr_2O_3 (DCMA no. 12-25-5);[2,3]
- Pink corundum, Mn–Al_2O_3 (DCMA no. 3-04-5);[2]
- Pink coral zircon, Fe–$ZrSiO_4$ (DCMA no.14-44-5);[2]
- Red $CdSe_xS_{1-x}$ encapsulated in zircon structure;[4]
- Reddish-brown $Ce_{1-x}Pr_xO_2$ with fluorite structure.[4]

The only pigment that presents an intense red tonality is the cadmium sulfoselenide. The use of this compound is limited by its low thermal stability. It decomposes in oxidizing atmospheres at temperatures above 600 °C. Another dificultis is the high toxicity of the materials used in its manufacture.[4]

The iron(III) in the pink-coral zircon pigment experiences reduction at high temperature with formation of variable contents in Fe(II) which implies modification of the color. The obtaining of new non-toxic ceramic pigments with high temperature stability requires searching for new host structures and new synthesis methods involving less toxic materials, which must be still more economically profitable.

These materials can be replaced by refractory oxides as the yttrium and aluminum oxide, which generally have a low toxicity rating. The yttrium and aluminum perovskite structure exhibits a great thermal stability, chemical resistance, little is known concerning its properties, quality and possible applications in ceramic glazes.

The octahedral coordination[5] in the perovskite structure is appropriate for introducing the chromium(III) ions, modulating this octahedral environment towards a strong crystal field, providing the red color.

On the other hand the high temperature of synthesis (1400, 1500 °C) does not permite the presence of chromium(VI) ions which are toxic.

There are different manners of obtaining red hues. One way could be exemplified by the intensification of the

* Corresponding author.
E-mail address: carda@qio.uji.es (Y. Marinova).

0955-2219/02/$ - see front matter
PII: S0955-2219(02)00182-6

crystal field of the chromium(III) ion when it substitutes for aluminum(III), in the corundum structure (α-Al_2O_3). In this case, the electronic transitions between d-electron orbitals in the chromium have relatively high energy, thus producing red tonality.[6] The chromium(III) is in distorted octahedral configuration with the oxygen ions.[7] The effect of the ligand field strength on the resulting energy levels, designated by the spectroscopic terms $^4A_2$, $^4T_1$, $^4T_2$ and ^2E can be observed on the energy level diagram of the Cr(III) ion shown in Fig. 1.

The energy of the ^2E level changes very little with respect to the ground level $^4A_2$ when the strength of the field is increased, but the $^4T_1$ and $^4T_2$ levels change significantly. When white light passes through a crystal of ruby (Cr^{3+}:Al_2O_3), a portion of it with energy 2.2 eV corresponding to the energy difference between the $^4A_2$ and $^4T_2$ levels of Cr(III) is absorbed. Another portion of light with energy 3.0 eV is absorbed due to the excitation of the ion from $^4A_2$ to $^4T_1$. The absorption resulting from the first transition is in the yellow-green part of the visible spectrum and the one from the second transition is in the violet part (see Fig. 1). Because of the vibration interactions, broad bands which overlap partially take place in the absorption spectrum. Thus the transmission in the blue region is weaker, and the absorption in the red region (energies below 2 eV), falls down to zero providing the red color of the ruby.

The ideal perovskite structure with general formula ABO_3, has a cubic face-centered structure, the smaller B cation occupying octahedral sites and the larger A ion occupying cubic sites (see Fig. 2).

Relatively few compounds present the ideal cubic perovskite[8] structure and slightly distorted structures with inferior symmetry are observed usually (included the mineral perovskite $CaTiO_3$). In the case of the neodymium perovskite $NdAlO_3$, the structure is trigonal and in the case of the yttrium perovskite $YAlO_3$ it is orthorhombic.[9]

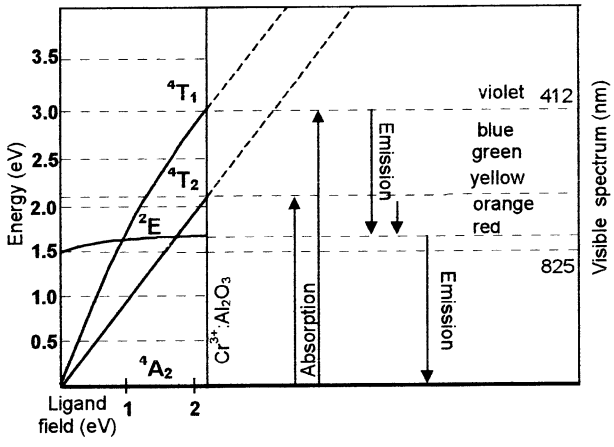

Fig. 1. Energy diagram of Cr^{3+} in octahedral ligand field.

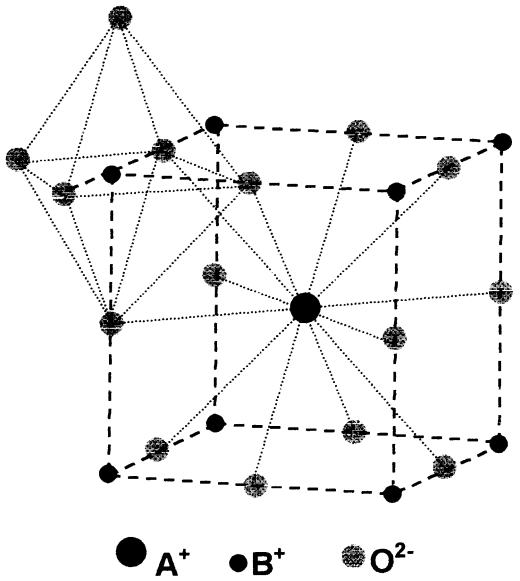

Fig. 2. Idealized cubic unit cell of the perovskite structure.

The purpose of the present study has been to synthesize the perovskite[4] $NdAlO_3$ and its solid solutions with Y^{3+} and Cr^{3+} ions employing ceramic and coprecipitation routes. The effect of different mineralizers, as well as the thermal stability of the obtained pigments in different enamels have been studied.

2. Experimental

2.1. Materials and methods

In order to decrease the synthesis temperatures of the studied systems, several mineralizers were selected. A mineralizer is a chemical agent that acts even in small concentrations to accelerate the physical–chemical transformations during the reaction processes in the solid state and affects particularly the reaction speed.

The mineralizer systems used for the present study are indicated in the Table 1, making reference to the origin of the components as well as to the percentage in respect to the total quantity of the sample.

These mineralizers, were selected as being the most usual systems used in the synthesis of ceramic pigments.

Table 1
Mineralizer systems with their references and used percentages

Reference	Mineralizer system/Wt. relation	Wt.% on the sample
M1	$H_3BO_3^a + Li_2CO_3^a/3 : 2$	5
M2	Criolita[b], Na_3AlF_6[b]	3
M3	$NaF^a + MgF_2^a + Li_2CO_3^a/3 : 2 : 1$.[a]	6

[a] Merck Farma y Química, S.A.
[b] QUIMIALMEL, S.A., España.

Table 2
Prepared nominal compositions via solid state reaction, together with their references

Nominal composition	Reference
$Y_{0,95}Nd_{0,05}Al_{0.95}Cr_{0,05}O_3$	1K
$YAI_{0,95}Cr_{0,05}O_3$	2K
$NdAIO_3$	3K

The nominal compositions prepared by the ceramic route are detailed in Table 2. The composition 3K was used to determine the most adequate mineralizer for the synthesis.

The precursors used for the preparation of the compositions are indicated in Table 3.

The flow diagram of the procedure followed in the preparation of the samples via solid state reaction is presented in Fig. 3.

As indicated in Fig. 3, the precursor oxides were mixed in a planetary ball mill (model "Fritz-Pulerisette") for 15 min, using acetone as a dispersion media. Subsequently, the acetone was evaporated at room temperature.

Table 3
Used precursors in the ceramic method[a]

Precursors	Purity
Nd_2O_3	95
Al_2O_3	99.5
Cr_2O_3	99
Y_2O_3	99

[a] Quimialmel S.A. Castellón (España).

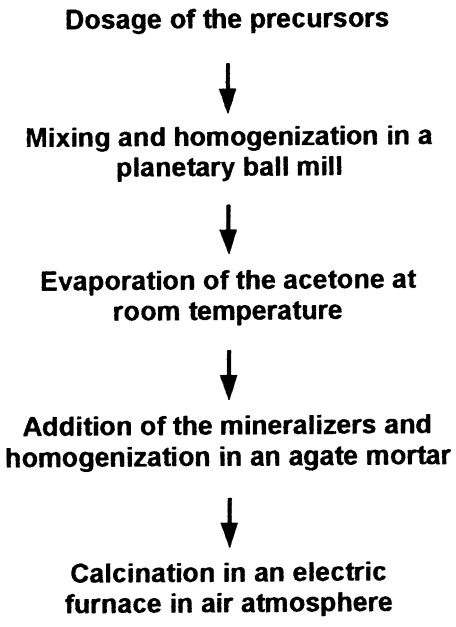

Fig. 3. Flow diagram of the procedure used for the preparation of the samples by solid state reaction.

The compositions of the samples prepared via coprecipitation are indicated in Table 4, together with the references used along the work.

The soluble salts used as precursors in the coprecipitation route are indicated in Table 5, except for the case of the Nd^{3+}, in which neodymium oxide was dissolved in acetic acid.

For the preparation of the samples, stoichiometrical quantity of the neodymium oxide was introduced in an aqueous solution of acetic acid while continuously stirring and heating at 70–80 °C until a completely transparent solution was obtained. The water–acetic acid ratio was H_2O:$CH_3COOH = 0.5$:1. The flow diagram of the coprecipitation process is presented in Fig. 4.

After being weighed, each precursor was dissolved in 50 ml of distilled water, stirring for 1 h, at 70–80 °C. Further on, all the solutions were mixed and stirred during 30 min in order to obtain a homogeneous solution. Adding ammonia (concentration 30%) drop by drop provoked destabilization of the system,[10] and a precipitate formed. This precipitate was dried under an infrared lamp.

Once dry, the samples prepared by both routes were homogenized with the selected mineralizers in an agate mortar and then heat treated in a NANETTI furnace. The maximum temperatures were between 1400 and 1500 °C for the ceramic route, and between 1300 and 1400 °C for the coprecipitation, reached with a heating rate of 10 °C/min. The maximum temperature was retained for 6 h, and the samples were left to cool freely in the furnace.

In order to evaluate the coloring capacity as well as the stability of the synthesized samples, they were introduced in two industrial enamels. One transparent enamel for biscuit substructes for application at 1080 °C and another transparent one for stoneware tile for 1200 °C, introducing in all cases 5 wt.% pigment in the enamel. The mixture was milled in water media for 10 min thus obtaining a suspension with a density of 1.6

Table 4
Prepared nominal compositions via coprecipitation, together with their references

Nominal composition	Reference
$Y_{0,95}Nd_{0,05}Al_{0,95}Cr_{0,05}O_3$	1C
$YAl_{0,95}Cr_{0,05}O_3$	2C

Table 5
Precursors used in the via coprecipitation

Precursor	Purity	Origin
$Y(NO_3)_3.9H_2O$	98.0 wt.%	Merck Farma y Química, S.A.
Nd_2O_3	95 wt.%	Quimialmel S.A. (España)
$AI(NO_3)_3.6H_2O$	98.0 wt.%	Merck Farma y Química, S.A.
$CrN_3O_9.9H_2O$	98.0 wt.%	Merck Farma y Química, S.A.

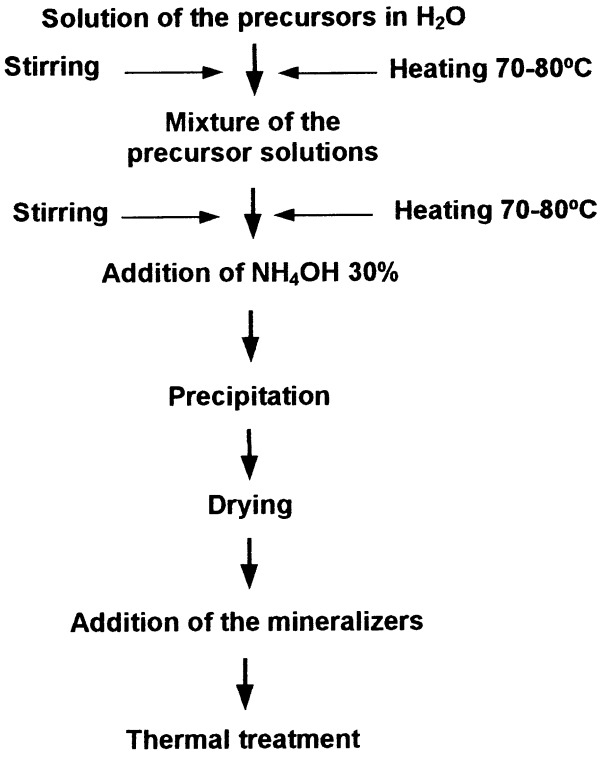

Fig. 4. Flow diagram of the coprecipitacion route.

kg/l. This suspension was applied on the surface of the ceramic supports, totally covering them with a homogeneous layer.

3. Characterization techniques

3.1. X-ray diffraction

For the structural characterization of the synthesized materials, an X-ray diffractometer Siemens D5000, provided with a copper cathode was used. The measurements were performed in the interval of 20–60° 2θ with goniometer speed of 0.05° 2θ/s and the time for collection of the counts on every step was 1 s.

3.2. Electron microscopy

All synthesized materials were characterized microstructurally by means of scanning electron microscopy (SEM) on a LEO 440 microscope coupled with a spectrometer for energy dispersive X-ray analysis (EDAX). The range of signal collection was within the interval of 2.5–15 KeV.

3.3. Fluorescent emission spectroscopy

The emission measurements were carried out at ambient temperature exciting the samples with a Nd:YAG impulse laser emission at 530 nm (Jobin-Yvon) and detecting the fluorescence with an Optical Multichanel Analyzer (O.M.A.—EG&G) in the laboratories of the CNRS center of the University "Pierre et Marie Curie" (Paris).

3.4. Absorption measurements

The absorption spectra in the interval 400–800 nm and the CIE-Lab color[11] coordinates of the enameled ceramic tiles were obtained by a spectrofotometer Perkin-Elmer, Lambda-19. A pellet of MgO was used as a white reference. The data was treated with the software package PECOL (Version 2.01).

4. Results and discussion

4.1. Study of the mineralizer system

The most appropriate mineralizer system was selected by studying the composition, 3K, without doping. The analysis of the thermal evolution of the synthesized materials carried out by means of X-ray diffraction (XRD) showed that a firing temperature of 1000 °C and a retention time of 6 h were not enough to form the perovskite structure. Therefore, the same composition (3K) was submitted to a second thermal treatment at 1100 °C during 6 h.

The XRD measurements showed (Fig. 5) that when the mineralizer, M1, was introduced, a small quantity of the perovskite phase was formed, dominated by the peaks of the unreacted oxides. With the mineralizer system M2, the $NdAlO_3$-perovskite peaks in the diffraction patterns became more intense, but still with the peaks of the unreacted oxides. The purest phase appears to form in the case of using the mineralizer system M3,

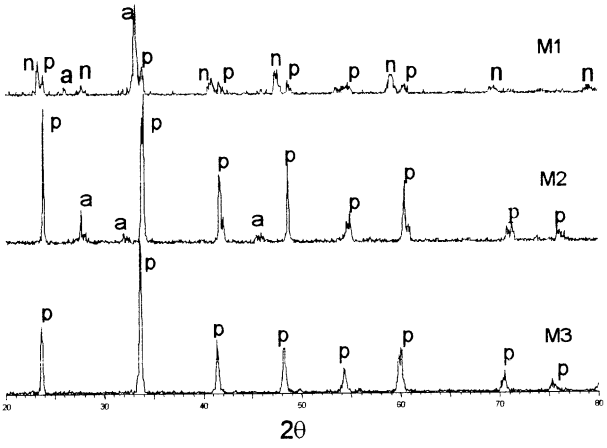

Fig. 5. XRD patterns of the sample referenced as 3K prepared with the mineralizers M1, M2 and M3 at 1100 °C/6h; p: perovskite phase, a: aluminum oxide and n: neodymium oxide.

when the perovskite peaks were most intense. These data seem to indicate the important role of the type of the selected mineralizer for the development of the neodymium aluminate. The beneficial effect of the selected mineralizers can be attributed to the development of liquid phases at relatively low temperatures facilitated by the presence of the alkaline agents, thus favoring the diffusion processes during otherwise solid state reaction.[12]

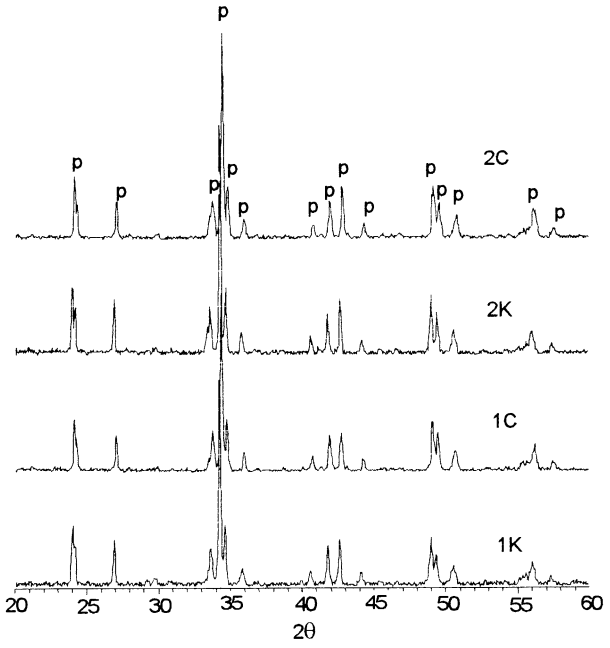

Fig. 6. XRD patterns of the sample synthesized via solid state reaction and coprecipitation; p: perovskite phase.

Considering these results, the most suitable mineralizer system was selected, for the series of doped samples (references 1K, 2K, 1C and 2C). The samples prepared by solid state reaction (1K and 2K) and coprecipitation (1C and 2C), with the mineralizer M3 added were submitted to the corresponding calcination cycles and then analyzed by means of XRD. The diffraction patterns are shown in Fig. 6.

These diffraction patterns show that the perovskite solid solution was not formed below a firing temperature of 1300 °C in either of the two synthesis routes. Only when the sample 1K was fired at 1400 °C during 6 h, the formation of the perovskite structure was observed. In the composition 2K the same structure appeared only just when fired at 1500 °C during 6 h. In the sample 1C obtained by the coprecipitation method the perovskite structure was formed after calcining at 1300 °C during 6 h. In the composition 2C the solid solution phase appeared after firing at 1400 °C during 6 h (Fig. 6). It must be pointed out that all the synthesized samples presented shades of red color.

The microstructure of the synthesized samples 1K and 1C, is illustrated by the SEM micrographs shown in Fig. 7.

It can be pointed out in the representative case of the sample 1K prepared by the solid state reaction that it consists of grains with a high degree of sintering, whose sizes vary between 1 and 3 m. In the case of the sample

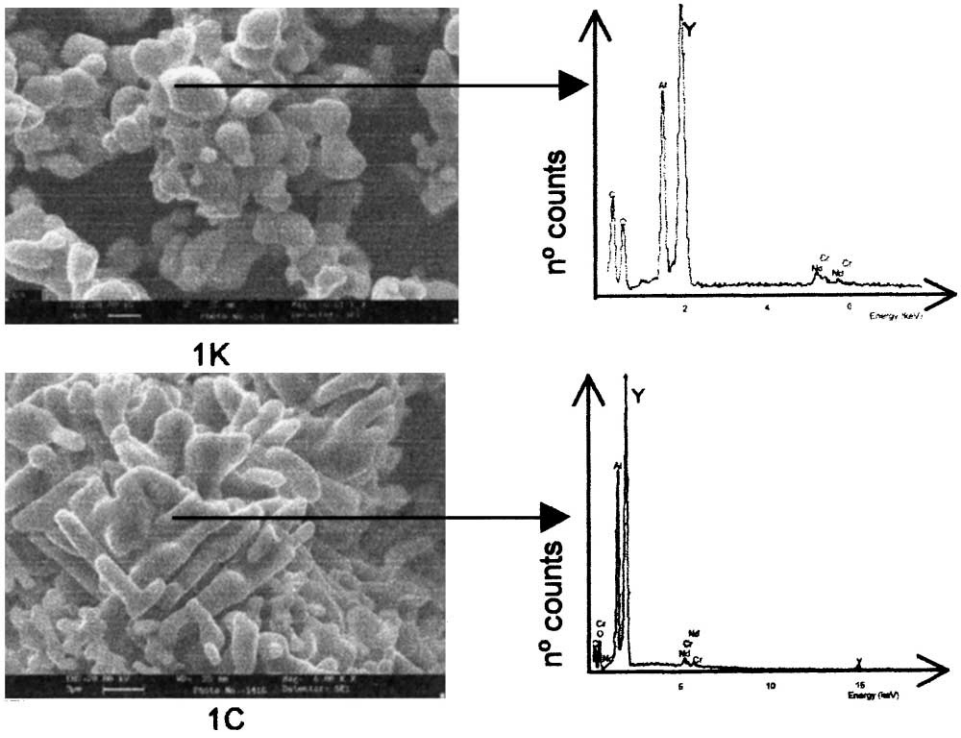

Fig. 7. SEM micrographs of the samples 1K (1400 °C/6h) and 1C (1300 °/6h) together with the spot chemical analysis.

1C prepared by coprecipitation, very sintered agglomerates are observed on the micrography. The homogeneity of the samples synthesized via the coprecipitation route was checked by the spot analysis and "mapping". It is observed that the percentile distribution of elements in the surface of the grains is nearly constant (Fig. 7).

However, the spot analysis in the samples synthesized by the solid state reaction, indicates small compositional variations between the different grains (Fig. 7). This fact could be explained by the low reactivity in this synthesis route related to the low diffusion degree of the different reactant ions.

4.2. Measurement of the optical properties: absorption and emission spectra

All solid solutions were analyzed by UV-Vis spectroscopy in order to study the surrounding of the Cr^{3+} chromophor. The spectra corresponding to the synthesized samples are presented in Fig. 8.

The theory of the ligand field,,[13] for an Cr(III) ion in an octahedral environment predicts the existence of three absorption bands. The energies of the first two electronic spin allowed transitions, $^4A_2 \rightarrow {}^4T_1$ and $^4A_2 \rightarrow {}^4T_2(F)$, correspond to visible light energies. The third spin allowed transition is the one from $^4A_2$ to $^4T_1$ (proceeding from the 4P state of the free ion); its energy corresponds to ultraviolet light, and therefore it doesn't affect the color. As can be observed on the absorption spectra of the obtained solid solution (Fig. 8), at wavelength values smaller than 580 nm, there is a region of nearly constant absorption, probably owing to matrix effects and the distinction of the bands assigned to the allowed transitions of the Cr^{3+} is impeded. It is also necessary to indicate that no absorption band appears in the visible spectrum between 610 and 700 nm (in the red region), contrary to the spectrum of the chromium(III) oxide where a wide absorption band can be appreciated in the same region. Considering the absorption spectra of the synthesized samples it can be concluded that the determination of the environment of the Cr^{3+} chromophore is a quite complex task. The emission spectroscopy technique gave better results in this respect.

The low energy levels for the $3d^3$ electronic configuration of the ion Cr^{3+}, in an octahedral environment are shown in Fig. 9 as a function of the crystal field.[13]

The luminescent processes of the Cr^{3+} can be explained using this same diagram including the energy levels $^4T_2$, ^2E and the fundamental one $^4A_2$.

In the well-studied glasses and glazes doped with Cr^{3+} the relation Dq/B varies in the interval from 2.0 to 2.8 eV and the energy gap ΔE between the levels $^4T_2$ and ^2E is in the range $-1200 \div 2300$ cm^{-1}. It can be observed that the level ^2E practically does not depend on the strength of the crystal field the variation of the value ΔE being only due to the change of the position of the level $^4T_2$. As can be seen in Fig. 9, in the cross point of the ^2E and $^4T_2$ energy levels, the value Dq/B≈2.2 and the difference ΔE between the energy levels is zero. The area on the right of this point corresponds to the values of the Dq/B parameter of a strong crystal field and the energy difference is $\Delta E > 0$. The area on the left of the crossover point corresponds to the lower values of the Dq/B parameter, where the Cr^{3+} ions are in crystallographic sites with a low crystal field ($\Delta E < 0$).

The electronic transitions of Cr^{3+} (for example Cr^{3+} in ruby) in a strong crystal field from the fundamental level to higher energy levels are indicated in Fig. 10.

The selection rules do not allow the relaxation directly from these levels to the fundamental level, but the transition from both levels to the intermediate level ^2E occurs almost immediately.[7,14,15] These transitions imply the emission of 1.2 eV radiation (relaxation from the level $^4T_1$) and 0.4 eV radiation (relaxation from $^4T_2$). These energies correspond to infrared radiation and the transitions are non-radiative. The relaxation of ^2E to the fundamental level implies an emission of 1.79 eV that coincides with the end of the red region of the visible spectrum and the production of red fluorescence. The

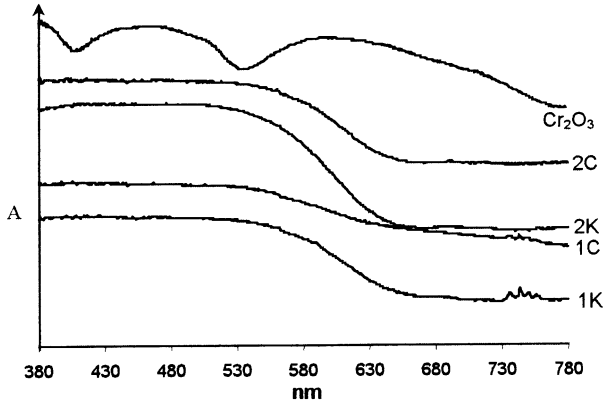

Fig. 8. UV-Vis spectrum of the samples obtained by ceramic and coprecipitation methods.

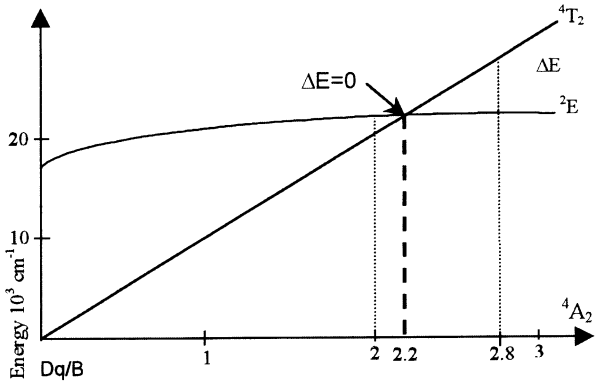

Fig. 9. Diagram of the low-lying energy levels of Cr^{3+} ions ($3d^3$) in octahedral coordination.

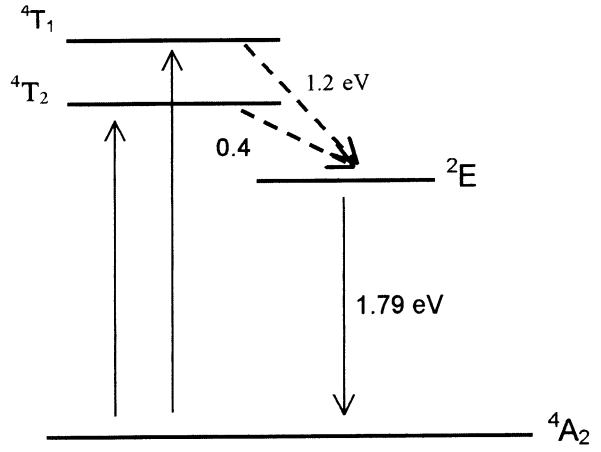

Fig.10. Energy levels of the Cr^{3+} ion in the ruby and illustration of the emission process.

produced fluorescence is not observed in normal conditions, but it has a significant contribution to the color. In fact, the red fluorescence consists of one or two very close lines at approximately 690 nm, called R lines.

They can be also observed in the emission spectra obtained at ambient temperature, of the samples presented in Fig. 11.

As can be appreciated in Fig. 11, the R lines appear approximately at 690 nm and they originate from the transition between the excited state ^2E and the fundamental state $^4A_2$. A splitting is observed that may be due to fragmentation of the ^2E state at lower symmetry of the crystal field. Also in most of the minerals and glasses, the Cr(III) is in octahedral coordination, however, the octahedron is usually deformed. Thus in the series of solid solutions, such distortion causes transition from cubic to orthorhombic symmetry. It should be

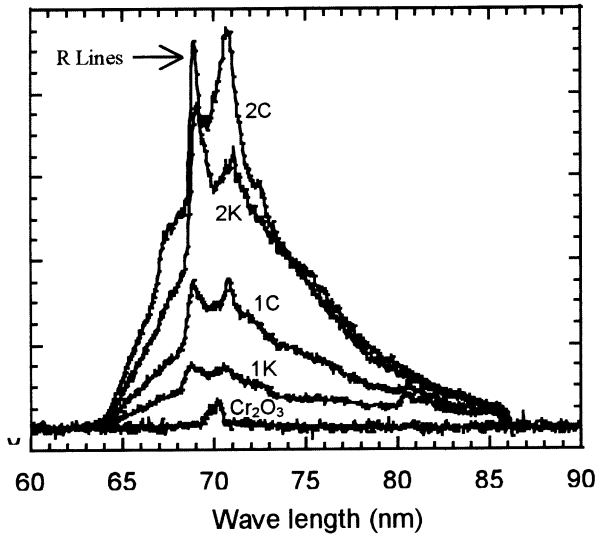

Fig. 11. Luminescence spectrum of Cr^{3+} of the sample at room temperature.

indicated that in glasses with $\Delta E > 0$, the radiative relaxation time in the excited state is dominated by the time of radiative relaxation of the ^2E metastable level and the extension of the population of the superior level $^4T_2$.

In ruby, as in the case of the synthesized samples, the strong crystal field situation (red color) is realized, and the ^2E level has lower energy at ambient temperature, the time of the radiative relaxation being controlled practically by the transition $^2E \rightarrow {}^4A_2$, that is to say it is the dominant one. The fluorescence intensity of the Nd^{3+}-doped samples (1K and 1C) (see Fig. 11) is lower than the fluorescence intensity samples that do not contain Nd^{3+}. This can be explained by an incomplete energy transfer[16] of Cr(III) to Nd(III) as it is shown in Fig. 12.

The bandwidth (transition $^4T_2$ to $^4A_2$) is too large for overlap from the absorption lines of rare earth ions such as the Nd^{3+} to occur. Incomplete energy transfer $Cr^{3+} \rightarrow Nd^{3+}$ can be appreciated in Fig. 12 expressed as the overlap of the Cr^{3+}-emission and the Nd^{3+}-absorption. The arrow, in the same figure indicates the electronic transfer.

Therefore, the red color that develops in the samples can be explained by both the spectral absorption and an additional contribution from the fluorescent emission.

4.3. Application of the synthesized structures as ceramic pigments

The color measurements on the enameled tiles colored with the synthesized pigments evidence the absence of defects that could be caused by the enameling process. All enameled samples present stable red hues. It can be seen from Table 6, that the highest red component (the highest value of the co-ordinate a*) is reached in the enameled tiles colored with the pigments 2K and 2C.

The applicability of these materials as red pigments in color ceramic glazes of low (1080 °C) and high (1200 °C) temperature was tested.

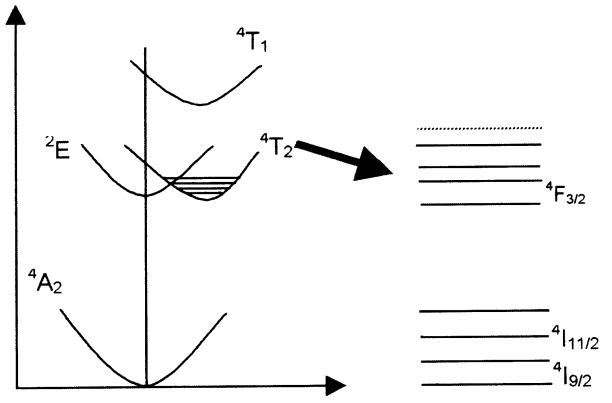

Fig. 12. Energy level diagram of the donor (Cr^{3+})–acceptor (Nd^{3+}). The electronic transfer is indicated with arrows.

Table 6
Chromatic coordinates CIE-La^*b^* of the enamel ceramic pigments

References	Enamel temperature (°C)	L^*	a^*	b^*
1K 1400 °C6	1080	39.60	25.39	16.88
1C 1300 °C6	1080	39.01	22.58	19.17
2K 1500 °C6	1080	43.63	27.92	21.92
2C 1400 °C6	1080	37.65	26.64	17.11
1K 1400 °C6	1200	43.48	22.89	18.13
1C 1300 °C6	1200	54.65	17.18	16.93
2K 1500 °C6	1200	48.92	26.21	20.24
2C 1400 °C6	1200	51.86	19.60	16.97

5. Conclusions

The following conclusions can be drawn from the obtained results:

1. The most appropriate mineralizer system for the formation of the $NdAlO_3$ perovskite in the given experimental conditions was the one consisting of: $NaF + MgF_2 + Li_2CO_3$ (3:2:1 by weight).

2. The solid solutions $Y_{0.95}Nd_{0.05}Al_{0.95}Cr_{0.05}O_3$ and $YAl_{0.95}Cr_{0.05}O_3$ were synthesized by coprecipitation and solid state reaction using the selected mineralizer system.

3. The solid solutions were obtained at lower temperature via the coprecipitation route.

4. The obtaining of the red color was studied in the perovskite solid solutions and the mechanism of its appearance was suggested on the base of the emission spectra of the materials.

5. The possibility of the application of these materials as red ceramic pigments for the ceramic industry was discussed.

Acknowledgements

The authors are grateful to: Agencia Española de Cooperación Internacional (Spain), Empersas: QUIMIALMEL S.A., Castellón y ESMALTES S.A., Alcora (Spain), Servicios Centrales de Instrumentación Científica, Universitat JAUME I (Spain).

References

1. Emiliani, G. P. and Gorbara, F., *Tecnologia Ceramica: Le Materie Prime*. Editoriale Faenza Editrice S.A., 1999, pp. 162–165.
2. *DCMA Clasification and Chemical Description of the Mixed Metal Oxide Inorganic Colored Pigments*, 2nd edn. Metal Oxides and Ceramic Colors Subcommitee. Dry Color Manufacturer's Assn, Washington, DC, 1982.
3. Stefani, R., Longo, E., Escribano, P., Cordoncillo, E. and Carda, J. B., Developing a pink pigment for glases. *Am. Ceram. Soc. Bull.*, 1997, **76**(9), 61–64.
4. Rincon, J., Ma Carda, J. and Alarcón, J., *Nuevos productos y tecnologías de esmaltes y pigmentos cerámicos*. Faenza Editrice Ibérica S.L, Castellón, 1992.
5. Alarcón, J. and Glasser, F. P., Yttrium aluminate garnets doped with chromium manganese and vanadium. *J. Mater. Csi Let.*, 1988, **7**, 187–190.
6. Chiang, Y. M., BirnieIII, D. and Kingery, W. D., *Physical Ceramics. Principles for Ceramic Science and Engineering*. John Wiley & Sons, New York, 1997.
7. Nassau, K., *The Physics and Chemistry of Color The Fifteen Causes of Color*. John Wiley & Sons, New York, 1983.
8. Borg, R. J. and Dienes, G. J., *The Physical Chemistry of Solids*. Academic Press, USA, 1991.
9. Kanke, Y. and Navrotsky, A., A colorimetric study of the lanthanide aluminium oxide and the lanthanide gallium oxides: stability of the perovskites and the garnets. *J. Solide State Chem.*, 1998, **141**, 424–436.
10. Kakihana, M., Invited review sol-gel preparation of high temperature superconducting oxides. *J. Sol-Gel Sci. and Technol.*, 1996, **6**, 7–55.
11. CIE. *Recommendation on Uniform Color Spaces, Color Difference Equations, Psychometrics Color Terms*. Suplement no. 2 of CIE, Publ. no. 15 (E1–1.31 1971). Bureau Central de la CIE, Paris, 1978.
12. Kingery, W. D., Bowen, H. K. and Uhlmann, D. R., *Introduction to Ceramics*, 2nd edn.. John Wiley and Sons, New York, 1997.
13. Marfunin, A. S., *Physics of Minerals and Inorganic Materials*. Springer-Verlag, Berlin Heidelberg New York, 1979.
14. Tuller, H. L., *Wide-Gap Luminescent Materials. Theory and Applications*. Stanley R. Rotman. Kluwer Academic, USA, 1997.
15. West, A. R., *Basic Solid State Chemistry and its Applications*, 2nd edn. John Wiley & Sons, New York, 1984.
16. Pruss, D., Huber, G. and Beimowski, A., Efficient Cr^{3+} Sensitiezed Nd^{3+}: GdScGa-Garnet Laser at 1.06 μm. *Appl. Phys.*, 1982, **B 28**, 355–358.